Progress In Electromagnetics Research, PIER 100, 129–152, 2010

CRITICAL ANALYSIS OF MICROWAVE SCATTERING RESPONSE ON ROUGHNESS PARAMETER AND MOISTURE CONTENT FOR PERIODIC ROUGH SURFACES AND ITS RETRIEVAL

G. Mittal and D. Singh

Department of Electronics and Computer Engineering
Indian Institute of Technology Roorkee
Roorkee, (UK)-247667, India

Abstract—The main aim of this paper is to accentuate the sensitivity of correlation length 'l' as an important roughness parameter in quantifying the moisture content of bare soil surfaces with specular scattering. For this purpose, an indigenously designed bistatic scatterometer has been used to generate co-polarized specular data at X-band (10 GHz) with incidence angle varied from 30°–70° in steps of 10 degrees. The moisture and roughness conditions of the bare soil surface were changed under controlled conditions. Twenty seven experimental fields specified on the ground of different roughness and moisture conditions have been analyzed. Higher level of moisture content with larger correlation lengths was found to be more suitable for observing the effect of increasing rms height on specular scattering. Kirchhoff approach (KA) considered under the stationary phase approximation (SPA) has been used as an inversion algorithm with the application of genetic algorithm for the retrieval of soil parameters. A good agreement was observed between the experimental and retrieved values of soil moisture content (m_v) and roughness parameters (s and l).

1. INTRODUCTION

Quantitative measure of soil moisture has been a gruesome task in science community due to various complexities involved in estimating it through conventional methods at large scale. In spite of this, the importance of soil moisture as a key parameter in modeling the two-way interaction between land and atmosphere cannot be undermined.

Corresponding author: D. Singh (dharmfec@gmail.com).

At present, various remote sensing techniques subsist to measure a variety of surface parameters from meso scale to micro scale for the distribution of soil moisture content and surface roughness. Microwave remote sensing is a promising approach to assess the soil moisture because of its weather independent imaging capability and sensitivity towards the dielectric and geometric properties of objects.

Experimental measurements, indoor or outdoor, play a primordial role in investigating new remote sensing methods and in validating surface and volume scattering models. Over the past few decades, a great amount of work done in this direction is centered primarily on the backscattering of electromagnetic fields from rough surfaces. Though, these investigations helped in improvement of the theoretical models for accurate assessment of surface parameters on one hand and in development of empirical and semi-empirical models on the other hand [1–3]. Still the uncertainties in segregation of surface roughness and soil moisture and their retrieval with single scattering coefficient exist. Taking it into account, polarimetric behavior of radar waves that gives information about the orientation and shape of the targets can serve as a useful tool in developing soil moisture retrieval algorithms. Amongst the numerous published works only few are oriented toward using bistatic polarimetric radar data for estimation of earth's parameters [4, 5].

A limited number of controlled experimental measurements have been performed for the forward scattering case. In a view of deficiency of data aimed at the investigation of the bistatic active remote sensing, few outdoor bistatic measurements have been reported [6]. Three substantial indoor experiments have been carried in the recent past [7, 8]. The first one was achieved by Roger De Roo (1996), where different rough surfaces with constant soil moisture have been measured at X-band and validated to different surface scattering models. Three different rough surfaces with constant soil moisture were measured at different frequencies and validated against different scattering models by Macelloni et al. in 2000. Kais Ben Khadra (2008) used a specular algorithm to estimate two surface roughnesses (smooth and rough). A new technique using coherent term of the Integral equation method (IEM) for estimating surface roughness was also presented in the thesis. However, these studies did not include the correlation length along with rms height for describing the roughness of the surface. Except for few reported works [9–11, 20], correlation length has not been considered properly so far in moisture retrieval studies due to its highly variable nature and difficulty in interpreting.

Hereby, in the present paper an effort is made to study the role of correlation length on specular scattering with changing parameters (i.e., rms height and moisture content). Stationary phase approximation (SPA) has been used as the inversion algorithm with genetic algorithm applied as an optimization technique for the retrieval of soil parameters (m_v, s and l). Genetic Algorithm (GA) has been applied in many engineering areas for optimized selection and simulation. It has advantages over traditional non-linear solution techniques that cannot always achieve an optimal solution [12]. A good agreement between the experimental and retrieved values has been observed with permissible amount of rms error.

This paper is divided into five sections. Section 2 describes the methodology with its sub-sections consisting of experimental description and measurements. Scattering model used for retrieval and the optimization algorithm are discussed in Section 3. Section 4 comprises of results and discussions and conclusion is finally reported in Section 5.

2. METHODOLOGY

2.1. Experimental Description

2.1.1. Experimental Set Up

An indoor bistatic measurement in specular direction was accomplished with the help of an indigenously designed scatterometer [5]. Scatterometer was configured to operate at X-band (10 GHz). Dual polarized pyramidal horn antennae served the purpose of generating co-polarized microwave data with incidence angles varied from 30° to 70° incrementing ten degrees at each step. External calibration of the scatterometer was done using square aluminium sheet of known radar cross section as the calibration target [13]. System parameters are mentioned in Table 1.

Table 1. System parameters.

Central frequency	10 GHz
Antenna gain	20 dB
Antenna type	Dual polarized pyramidal horn
Beam width for H-plane	17°
Beam width for E-plane	22°
Platform Height	3 m
Cross pol isolation	40 dB
Size of Al sheet	$2 \times 2\,\mathrm{m}^2$

2.1.2. Data Set

Test bed of dimensions 2 m $\times$ 2 m of bare sandy soil was prepared to carry out the experiment. An indigenously designed wooden spiked harrow has been used to generate periodically rough surfaces [14]. Harrows are designed such that by changing the depth of the spikes, vertical height could be varied and on changing the spacing between the spikes, horizontal roughness could be varied. In order to analyze the effect of correlation length on moisture and rms height, twenty seven soil fields have been prepared as mentioned in Appendix A. Nine moisture levels (0.072–0.2280 $\mathrm{cm}^3\ \mathrm{cm}^{-3}$) with each moisture level corresponding to three correlation lengths and five rms heights (0.40–0.88 cm) have been considered. Thus, a total of 135 data sets were acquired, each consisted of measuring σ° at two polarizations and five incidence angles; hence total number of measurements was 1350.

2.2. Experimental Measurements

2.2.1. Surface Roughness Measurements

Spread of heights about the reference surface is best described by the standard deviation of surface height variations (or rms height, s). A surface in the x-y plane whose height at point (x, y) is $s(x, y)$ above the x-y plane can be characterized by its mean height $\bar{s}(x, y)$. If $s(x, y)$ is statistically independent of the azimuth angle in the x-y plane, then it is sufficient to use $s(x)$ alone to characterize the statistical properties of the surface [1]. The standard deviation of the surface height s is given in terms of $\bar{s}$ and the second moment $\overline{s^2}$

$$RMS_{height} = s = \left(\overline{s^2} - \bar{s}^2\right)^{1/2} \tag{1}$$

The variation of heights along the surface is given by the correlation length, l that acts as a reference in estimating the statistical independence of the two points on the surface. If the two points on the surface are separated by a horizontal distance greater than l, then their heights may be considered statistically independent of one another. The surface correlation function, $\rho(x')$ is a measure of degree of correlation between the height $s(x)$ at a point x and the height $s(x + x')$ at a point x' distance from x [1];

$$\rho\left(x'\right) = \frac{\int s\left(x\right) s\left(x + x'\right) dx}{\int s^2\left(x\right) dx} \tag{2}$$

The surface correlation length is defined as the displacement x' for which $\rho(x')$ is equal to e^{-1}

$$\rho(l) = 1/e \tag{3}$$

A surface with a rapidly varying height profile has a short value for l, whereas for perfectly smooth surface for which any point is perfectly correlated with every other point, l is infinite. In general, the rms height s is a measure of the vertical roughness of the surface and $1/l$ is a measure of the horizontal roughness. The two main forms of the surfaces are exponential and Gaussian, formulated as:

$$\rho_1\left(x'\right) = \exp\left(-x'^2/l^2\right)\ldots\text{Gaussian} \tag{4}$$

$$\rho_2\left(x'\right) = \exp\left(-\sqrt{2}x'/l\right)\ldots\text{Exponential} \tag{5}$$

The height profiles of the soil surfaces were measured by the pin profilometer/pin meter. The pin meter uses evenly spaced pins held parallel to each other to determine a surface height profile for the length of the pin meter [15]. The surface profile thus obtained is used to calculate rms height and correlation length from Eqs. (1)–(4) with the help of Matlab software. Based on an analysis of the surface height distributions we concluded that the surface height deviation is approximately Gaussian for all the fields under study.

2.2.2. Soil Moisture Measurement

Soil moisture measurements were made by taking five soil samples for each moisture condition. Each sample was weighed and then dried at 110° in preheated oven for 10–12 hr and then weighed again. Gravimetric soil moisture content was calculated as given in Eq. (6) [16]

$$m_g = \frac{W_{moist} - W_{dry}}{W_{dry}} \tag{6}$$

where m_g is the gravimetric moisture content, W_{moist} is the weight of moist soil sample, W_{dry} is the weight of the dry soil sample. Soil bulk density was measured and multiplied by the gravimetric moisture content to obtain volumetric moisture content.

2.2.3. Scattering Coefficient Computation

The calibration of the system has been done using square aluminium sheet of known radar cross section. The radar cross section (RCS) of the aluminium sheet is calculated using following relation [13]:

$${}_{al}\sigma_{pp}(\theta) = \frac{4\pi A^2}{\lambda^2}\left[\frac{\sin(kb\sin\theta)}{kb\sin\theta}\right]^2\cos^2\theta, \quad p = v \text{ or } h \tag{7}$$

where, ${}_{al}\sigma_{pp}(\theta)$ is the RCS of Aluminium sheet, A is area of the sheet, λ is wavelength of operation, θ is angle of incidence, b is the dimension of square sheet, and $k = 2\pi/\lambda$.

Scattering coefficient (i.e., radar cross section per unit m^2) for soil ($_s\sigma_{pp}(\theta)$) is calculated using relation based on power scattered from aluminium sheet and soil at various incidence angles as:

$$ {}_s\sigma_{pp}(\theta) = \frac{{}_sP_{pp}}{{}_{al}P_{pp}} \times {}_{al}\sigma_{pp}(\theta), \quad p = v \text{ or } h \tag{8} $$

$_{al}P_{pp}$ is the scattered power form Al sheet and $_sP_{pp}$ is the scattered power from soil.

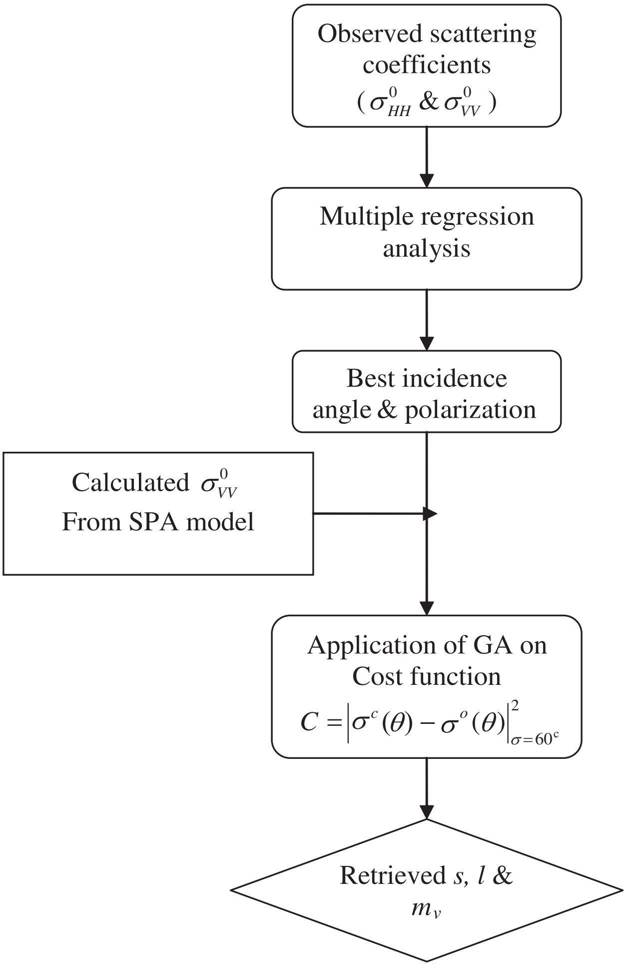

Figure 1. Flow chart for application of genetic algorithm on field data for retrieval of soil parameters.

3. RETRIEVAL ALGORITHM

Flow chart in Figure 1 summarizes the steps followed in retrieval of soil parameters (m_v, s and l). Experimental data is generated at different combinations of parameters (s, l and m_v). In second step multiple regression has been carried out for selecting the best incidence angle and the best polarization for observing the test fields. Finally GA is used for retrieval of surface parameters and soil moisture in which SPA model is used to generate cost function.

3.1. Kirchhoff Approach under Stationary Phase Approximation (SPA)

Kirchhoff approach or the tangent plane approximation requires additional simplifying assumptions in order to obtain analytic solution for the surface scattering problem. The stationary phase approximation or more widely known as the geometric optics approach assumes that scattering can occur only along directions for which there are specular points on the surface. For a rough surface with Gaussian height distribution, the incoherent scattering coefficient of the geometric optic approach is given by [1, 6, 7]:

$$\sigma_{pq}^0 = \frac{\left(kq \left|U_{pq}\right|^2\right)}{2q_z^4 \sigma^2 \left|\rho''(0)\right|} \exp\left[-\frac{q_x^2 + q_y^2}{2q_z^4 \sigma^2 \left|\rho''(0)\right|}\right] \tag{9}$$

where $\rho''(0)$ is the second derivative of the surface correlation function calculated at the origin, $\sigma^2|\rho''(0)|$ represents the mean square slope of the surface, U_{pq} is the complex coefficient which depends on the polarization, the relative dielectric constant and the specular angle. For specular direction Eq. (9) reduces to:

$$\sigma_{pq}^0 = \frac{\left|U_{pq}(\theta)\right|^2}{2\sigma^2 \left|\rho''(0)\right|}, \quad \text{where } p, q = h \text{ or } v \tag{10}$$

derivation of Eq. (10) is given in Appendix B.

Rms slope for gaussian surface is $\sqrt{2}\,(s/l)$ as mentioned in [2]. Through regression analysis, incidence angle of 60 degrees for VV polarization was found to be the best suitable incidence angle to study the effect of s, l and m_v on scattering coefficient in specular direction. Therefore, all the three parameters are retrieved using Eq. (10) for VV polarization at an incidence angle of 60°. For VV polarization $|U_{pq}|$ in Eq. (10) is replaced by $|U_{VV}|$ from Appendix B. The dielectric constant 'ε' in terms of volumetric moisture content was calculated using the empirical relation established by Topp et al., in 1980.

$$\varepsilon = 3.03 + 9.3m_v + 146m_v^2 - 76.7m_v^3 \tag{11}$$

This empirically determined third order polynomial expression for the dielectric constant is independent of type, bulk density, texture, salinity and temperature of the soil and is confirmed in several investigations [17].

3.2. Application of Genetic Algorithm for Retrieving Moisture Content and Roughness Parameters

Genetic algorithm is chosen as the optimization technique for retrieving soil parameters from nonlinear Eq. (10). Genetic algorithm is a probabilistic search approach which is founded on the ideas of evolutionary processes. An initial population is created containing a predefined number of individuals (or solutions), each represented by a genetic string (incorporating the variable information). Each individual has an associated fitness measure, typically representing an objective value. The concept that fittest (or best) individuals in a population will produce fitter offspring is then implemented in order to reproduce the next population. Selected individuals are chosen for reproduction (or crossover) at each generation, with an appropriate mutation factor to randomly modify the genes of an individual, in order to develop the new population. The result is another set of individuals based on the original subjects leading to subsequent populations with better (min. or max.) individual fitness. Therefore, the algorithm identifies the individuals with the optimizing fitness values, and those with lower fitness will naturally get discarded from the population [18].

3.3. Cost Function for GA

Three parameters s, l and m_v are encoded into genes to be optimized. Scattering coefficient for VV polarization 'σ^o_{VV}' (superscript "O" denotes observed) observed at 60° in specular direction is used to retrieve parameters. From the trial solutions of chromosomes in GA, 'σ^R_{VV}' (superscript "R" denotes retrieved) in SPA model is calculated and then used to form cost or fitness function as follows:

$$C = \sum_{\theta} \left|\sigma^c_{vv}(\theta) - \sigma^o_{vv}(\theta)\right|^2 \tag{12}$$

where $C = f(s, l, m_v)$ and θ is kept constant at 60°. Summation over the five observed incidence angles could create ambiguity in results and thus the best suitable incidence angle is only used for the purpose.

4. RESULTS AND DISCUSSIONS

4.1. Response of Specular Scattering Coefficient with Varying Roughness Parameters and Moisture Contents

Microwave measurements have been taken for both like polarizations (i.e., HH and VV polarization) in specular direction. Specular scattering coefficient has been computed for twenty seven fields at five incidence angles (30°–70° in steps of 10 degrees). Moisture conditions (volumetric) were varied from $0.072\,\text{cm}^3\,\text{cm}^{-3}$–$0.228\,\text{cm}^3\,\text{cm}^{-3}$ over soil bed whose roughness was varied so as to create moderately rough and rougher surfaces. Roughness conditions of the bare soil were varied in terms of correlation length (1.51 cm–2.97 cm) and rms height (0.40–0.88 cm).

Multiple and partial regression analysis was done in order to find the best suitable angle of incidence for studying the effect of s, l and m_v on specular scattering coefficient. Results of the analysis are mentioned in Table 2. From the table, it is obvious that composite effect of s, l and m_v on σ° and their individual effect (with the other two parameters held constant) are more profound at 60° for VV polarization with lower S.E.E.. The maximum value of coefficient of determination (i.e., R^2= 0.9089) is obtained at 60° incidence angle for VV polarization whereas maximum value of R^2 is 0.8022 at 50° for HH polarization. The coefficient of determination defines the percentage of dependence

Table 2. Multiple Regression results among ks, kl, m_v and scattering coefficient for various incidence angles at X-band (10 GHz). R is correlation coefficient, R^2 is coefficient of determination, r_l^2, r_m^2, r_s^2 are the partial coefficient of determination for l, m_v and s.

AOI	POL.	R	R^2	S.E.E.	r_l^2	r_m^2	r_s^2
30°	VV	0.7668	0.6396	2.1287	0.0429	0.0921	0.2533
40°	VV	0.8057	0.6492	1.8925	0.0099	0.0421	0.5759
50°	VV	0.7521	0.5657	2.8139	0.1285	0.0202	0.4832
60°	VV	0.9534	0.9089	1.4993	0.8915	0.8330	0.5245
70°	VV	0.9140	0.8354	1.8817	0.5663	0.7383	0.6023
30°	HH	0.7829	0.6130	2.0901	0.1951	0.3663	0.4461
40°	HH	0.8202	0.6727	2.0039	0.3658	0.5013	0.4841
50°	HH	0.8956	0.8022	1.5899	0.1897	0.0677	0.5352
60°	HH	0.7683	0.5904	1.5303	0.0001	0.2040	0.1037
70°	HH	0.6494	0.4217	1.4544	0.2865	0.2284	0.2446

Table 3. Dynamic Range for each moisture content and correlation length.

$\mathbf{m_v}$	**l**	**Dynamic range (dB)**	$\mathbf{m_v}$	**l**	**Dynamic range (dB)**	$\mathbf{m_v}$	**l**	**Dynamic range (dB)**
m_1	l_1	5	m_2	l_1	10.5	m_3	l_1	7.1
	l_2	3.5		l_2	8		l_2	8.2
	l_3	6.5		l_3	4		l_3	2.0
m_4	l_4	5.2	m_5	l_4	2.5	m_6	l_4	2.6
	l_5	9.5		l_5	4		l_5	5.3
	l_6	5.9		l_6	5.8		l_6	2.8
m_7	l_7	6.6	m_8	l_7	6.4	m_9	l_7	1.6
	l_8	8.5		l_8	5.2		l_8	7.2
	l_9	4		l_9	8.2		l_9	6.2

†where values of $m_{1\to 9}$ and $l_{1\to 9}$ are given in table of Appendix A.

of specular scattering on soil moisture and roughness parameters (for our case). Therefore, it infers that VV polarization at 60° may be the better option for retrieving the soil moisture and roughness parameter. Hence for further retrieval of surface parameters and soil moisture content, we have only considered VV polarization and not the HH polarization.

Figures 2(a_1)–(a_3) show the $\sigma°$ behavior with increasing rms heights at moisture levels $m_1 = 0.072\,\text{cm}^3\,\text{cm}^{-3}$, $m_2 = 0.077\,\text{cm}^3\,\text{cm}^{-3}$ and $m_3 = 0.086\,\text{cm}^3\,\text{cm}^{-3}$ at correlation lengths of 2.97 cm, 2.64 cm and 2.29 cm. At moisture level $m_1 = 0.072\,\text{cm}^3\,\text{cm}^{-3}$ as shown in Figure 2(a_1), for $l_1 = 2.97$ cm and $l_2 = 2.64$ cm, $\sigma°$ decreases at $s_2 = 0.46$ cm, increases at intermediate s values and again falls at $s_5 = 0.88$ cm. Dynamic range for l_1 and l_2 is 5 dB and 3.5 dB respectively as given in Table 3. However, for $l_3 = 2.29$ cm $\sigma°$ decreases with increase in s from $s_1 = 0.4$ cm to $s_5 = 0.88$ cm with a slight increase at $s_4 = 0.74$ cm. The dynamic range for l_3 is 6.5 dB. In Figure 2(a_2), at $m_2 = 0.077\,\text{cm}^3\,\text{cm}^{-3}$, dynamic range of $\sigma°$ for l_1 is 10.5 dB, 8 dB for l_2 and 4 dB for l_3. For l_1 and l_3, $\sigma°$ decreases with increasing s values, but for $l_2 = 2.64$ cm, an abrupt increase in $\sigma°$ values is observed at $s_2 = 0.46$ cm and $s_5 = 0.88$ cm. It is obvious from Figure 2(a_3) that for $m_3 = 0.086\,\text{cm}^3\,\text{cm}^{-3}$, $\sigma°$ decreases with increasing s at all the three correlation lengths. For $l_1 = 2.97$ cm and $l_2 = 2.64$ cm, dynamic range is 7.1 dB and 8.2 dB accordingly. For $l_3 = 2.29$ cm, scattering coefficient varies slightly and its dynamic range is 2 dB.

It can thus be concluded that for smallest correlation length (i.e., 2.29 cm) among the three, dynamic range is lower at moisture levels m_2 and m_3. It signifies that the variation in scattering coefficient with increasing roughness (in terms of s) is minimum at l_3.

Figures 2(b$_1$)–(b$_3$) show the response of σ° with increasing rms height at moisture contents $m_4 = 0.106\,\mathrm{cm}^3\,\mathrm{cm}^{-3}$, $m_5 = 0.121\,\mathrm{cm}^3\,\mathrm{cm}^{-3}$ and $m_6 = 0.129\,\mathrm{cm}^3\,\mathrm{cm}^{-3}$ respectively at three moderate correlation lengths, i.e., $l_4 = 2.15$ cm, $l_5 = 2.02$ cm and $l_6 = 1.86$ cm. At moisture level $m_4 = 0.106\,\mathrm{cm}^3\,\mathrm{cm}^{-3}$, irregularity in behavior of σ° with increasing s can be observed for the three correlation lengths under consideration (Figure 2(b$_1$)). For l_5 and l_6, σ° values fall nearer to each other with increasing s values from $s_1 = 0.4$ cm to $s_4 = 0.74$ cm. Dynamic range for $l_5 = 2.05$ cm is 9.5 dB and 5.9 dB for $l_6 = 1.86$ cm. For largest l, i.e., 2.15 cm, dynamic range is 5.2 dB. For $m_5 = 0.121\,\mathrm{cm}^3\,\mathrm{cm}^{-3}$, σ° decreases with increase in s values from $s_1 = 0.4$ cm to $s_5 = 0.88$ cm at l_4, l_5 and l_6 as obvious from Figure 2(b$_2$). For smaller correlation length, i.e., $l_6 = 1.86$ cm, σ° has higher values and least for l_5. For $l_4 = 2.15$ cm, σ° shows a constant

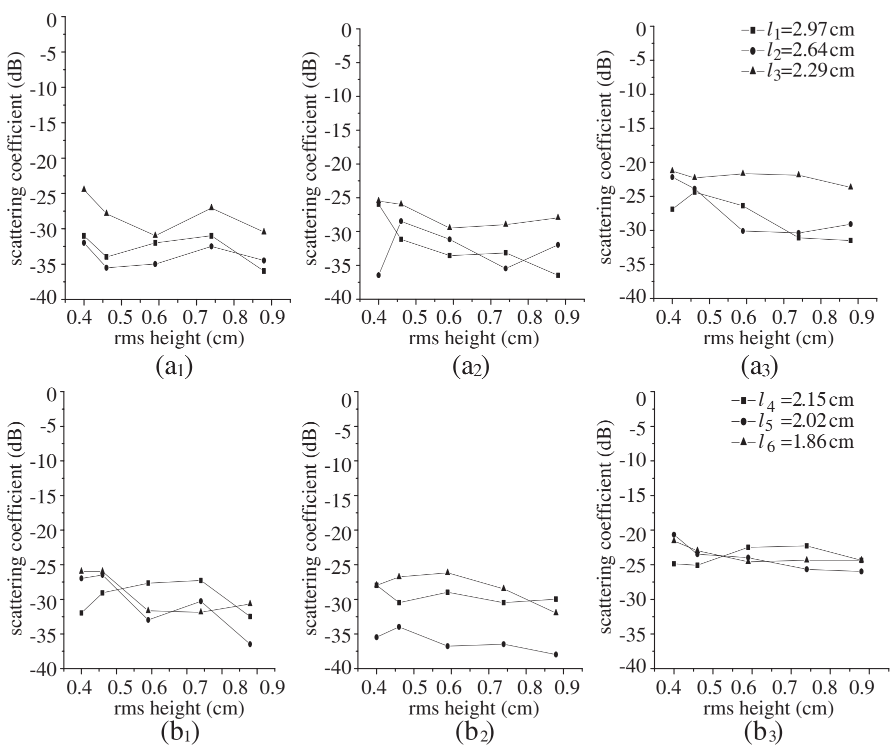

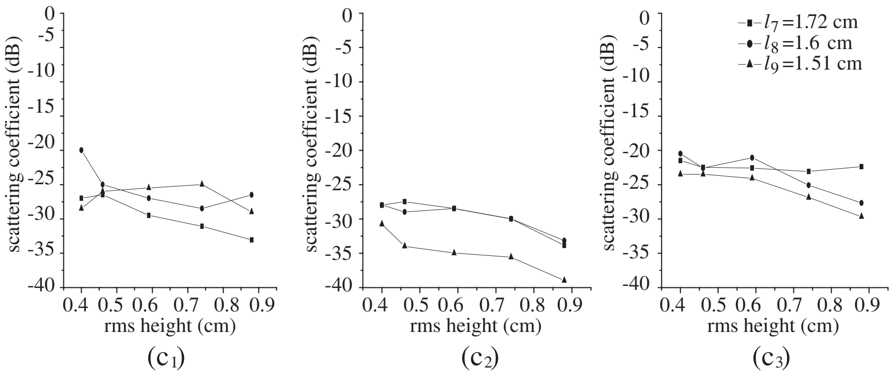

Figure 2. (a_1)–(a_3) Response of scattering coefficient with rms ht. at $m_1 = 0.072\,\mathrm{cm^3\,cm^{-3}}$, $m_2 = 0.077\,\mathrm{cm^3\,cm^{-3}}$ and $m_3 = 0.086\,\mathrm{cm^3\,cm^{-3}}$ respectively at correlation lengths $l_1 = 2.97\,\mathrm{cm}$, $l_2 = 2.64\,\mathrm{cm}$, $l_3 = 2.29\,\mathrm{cm}$. (b_1)–(b_3) Response of scattering coefficient with rms ht. at $m_4 = 0.106\,\mathrm{cm^3\,cm^{-3}}$, $m_5 = 0.121\,\mathrm{cm^3\,cm^{-3}}$ and $m_6 = 0.129\,\mathrm{cm^3\,cm^{-3}}$ respectively at correlation lengths $l_4 = 2.15\,\mathrm{cm}$, $l_5 = 2.02\,\mathrm{cm}$, $l_6 = 1.86\,\mathrm{cm}$. (c_1)–(c_3) Response of scattering coefficient with rms ht. at $m_7 = 0.169\,\mathrm{cm^3\,cm^{-3}}$, $m_8 = 0.184\,\mathrm{cm^3\,cm^{-3}}$ and $m_9 = 0.228\,\mathrm{cm^3\,cm^{-3}}$ respectively at correlation lengths $l_7 = 1.72\,\mathrm{cm}$, $l_8 = 1.60\,\mathrm{cm}$, $l_9 = 1.51\,\mathrm{cm}$.

decrease in values with a dynamic range of 2.5 dB. For $l_6 = 1.86\,\mathrm{cm}$, σ° tend to increase at intermediate values of s (i.e., s_2 and s_3), but decreases as roughness increases further to $s_5 = 0.88\,\mathrm{cm}$. The dynamic range for l_5 and l_6 is 4 dB and 5.8 dB respectively. As clear from Figure 2(b_3) at moisture level $m_6 = 0.129\,\mathrm{cm^3\,cm^{-3}}$, for $l_4 = 2.15\,\mathrm{cm}$, σ° remains almost constant with only a slight increase observed at $s_3 = 0.59\,\mathrm{cm}$ and $s_4 = 0.74\,\mathrm{cm}$. The dynamic range observed for l_4 is 2.6 dB. For l_5 and l_6, σ° values lie closer to each other for smaller s values (i.e., $s_1 = 0.4\,\mathrm{cm}$, $s_2 = 0.46\,\mathrm{cm}$ and $s_3 = 0.59\,\mathrm{cm}$). The dynamic range is 5.3 dB and 2.8 dB respectively for l_5 and l_6. Hence, it can be inferred from the discussion that larger correlation length among the selected combination of correlation lengths ($l_4 = 2.15\,\mathrm{cm}$, $l_5 = 2.02\,\mathrm{cm}$ and $l_6 = 1.86\,\mathrm{cm}$.) has lowest dynamic range (for m_5 and m_6) and at this particular value of l, effect of s on scattering coefficient is least.

Figures 2(c_1)–(c_3) show the response of scattering coefficient with increasing rms height, at moisture contents $m_7 = 0.169\,\mathrm{cm^3\,cm^{-3}}$, $m_8 = 0.184\,\mathrm{cm^3\,cm^{-3}}$ and $m_9 = 0.228\,\mathrm{cm^3\,cm^{-3}}$ respectively at three correlation lengths, i.e., $l_7 = 1.72\,\mathrm{cm}$, $l_8 = 1.60\,\mathrm{cm}$ and $l_9 = 1.51\,\mathrm{cm}$. At moisture level $m_7 = 0.169\,\mathrm{cm^3\,cm^{-3}}$, for larger correlation length

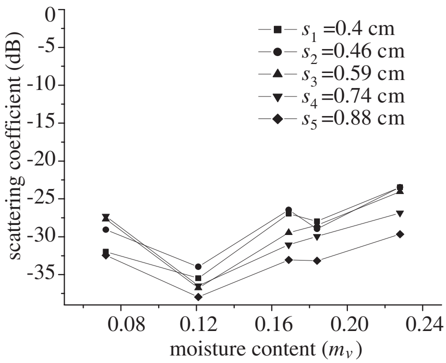

Figure 3. Response of σ° with increasing moisture content at different rms height.

of $l_7 = 1.72\,\text{cm}$, σ° shows a decreasing trend as s increases from $s_1 = 0.4\,\text{cm}$ to $s_5 = 0.88\,\text{cm}$ with dynamic range of 6.6 dB. However, σ° response for lower l values (i.e., $l_8 = 1.60\,\text{cm}$ and $l_9 = 1.51\,\text{cm}$) becomes irregular. For moisture content $m_8 = 0.184\,\text{cm}^3\,\text{cm}^{-3}$, σ° values for l_7 and l_8 are approximately same as s increases from $s_1 = 0.4\,\text{cm}$ to $s_5 = 0.88\,\text{cm}$. For $l_9 = 1.51\,\text{cm}$, σ° decreases as s increases from $s_1 = 0.4\,\text{cm}$ to $s_5 = 0.88\,\text{cm}$ with a dynamic range of 8.2 dB. As shown in Figure 2(c_3), at smallest l (i.e., 1.51 cm), σ° has lowest values which decreases further as s increases from $s_1 = 0.4\,\text{cm}$ to $s_5 = 0.88\,\text{cm}$. For higher l (i.e., $l_7 = 1.72\,\text{cm}$ and $l_8 = 1.60\,\text{cm}$), σ° has higher values. At $s_1 = 0.4\,\text{cm}$ to $s_3 = 0.59\,\text{cm}$, σ° values for l_7 and l_8 tends to coalesce but at higher rms height, i.e., $s_4 = 0.74\,\text{cm}$ and $s_5 = 0.88\,\text{cm}$, σ° values are lower for l_7 and higher for l_8. The dynamic range for l_7 is 1.6 dB being smallest in comparison to 7.2 dB and 6.2 dB for l_8 and l_9 accordingly. Thus, for largest correlation length, i.e., l_7 among the set of three correlation lengths, effect of increasing s on scattering coefficient is minimum at highest moisture level, i.e., $m_9 = 0.228\,\text{cm}^3\,\text{cm}^{-3}$.

In Figure 3, effect of increasing moisture content on scattering coefficient at five different values of s has been displayed. For each s value, scattering coefficient increases as the moisture content increases. At smaller values of s, i.e., $s_1 = 0.4\,\text{cm}$ to $s_3 = 0.59\,\text{cm}$, response of scattering coefficient with increase in moisture content is not much clearer as for higher values of s. For $s_4 = 0.74\,\text{cm}$ and $s_5 = 0.88\,\text{cm}$, as moisture content increases from $0.106\,\text{cm}^3\,\text{cm}^{-3}$ to $0.228\,\text{cm}^3\,\text{cm}^{-3}$, the response curves for both s values can easily be discriminated. An overall decrease in σ° values is observed as rms height increases irrespective of change in moisture level.

In Figures 4(a)–(c), a set of three moisture levels, $0.072\,\mathrm{cm}^3\,\mathrm{cm}^{-3}$, $0.077\,\mathrm{cm}^3\,\mathrm{cm}^{-3}$ and $0.086\,\mathrm{cm}^3\,\mathrm{cm}^{-3}$ for each of the correlation length 2.97 cm, 2.64 cm and 2.29 cm has been taken to see the behavior of σ° with increasing rms height. It is obvious from Figures 4(a), (b) and (c), that at the higher correlation length of 2.97 cm, response of σ° with rms height at different moisture levels is undistinguishable but as l lowers to 2.29 cm it gains regularity.

In Figures 4(d)–(f), σ° response at three different moisture levels (i.e., $m_4 = 0.106\,\mathrm{cm}^3\,\mathrm{cm}^{-3}$, $m_5 = 0.121\,\mathrm{cm}^3\,\mathrm{cm}^{-3}$ and $m_6 = 0.129\,\mathrm{cm}^3\,\mathrm{cm}^{-3}$) at three correlation lengths (2.15 cm, 2.02 cm and 1.86 cm) has been displayed. Figure 4(d) shows the response for moisture levels $m_4 = 0.106\,\mathrm{cm}^3\,\mathrm{cm}^{-3}$, $m_5 = 0.121\,\mathrm{cm}^3\,\mathrm{cm}^{-3}$ and $m_6 = 0.129\,\mathrm{cm}^3\,\mathrm{cm}^{-3}$ at higher correlation length of 2.15 cm. Figures 4(e) and 4(f) show the response at the same moisture levels for correlation lengths of 2.02 cm and 1.86 cm accordingly. As moisture level increases, σ° increases for each of the correlation length under consideration. Highest moisture level $m_6 = 0.129\,\mathrm{cm}^3\,\mathrm{cm}^{-3}$ amongst the three moisture levels under consideration, shows a better σ° response for each of the correlation length, i.e., 2.15 cm, 2.02 cm and 1.86 cm.

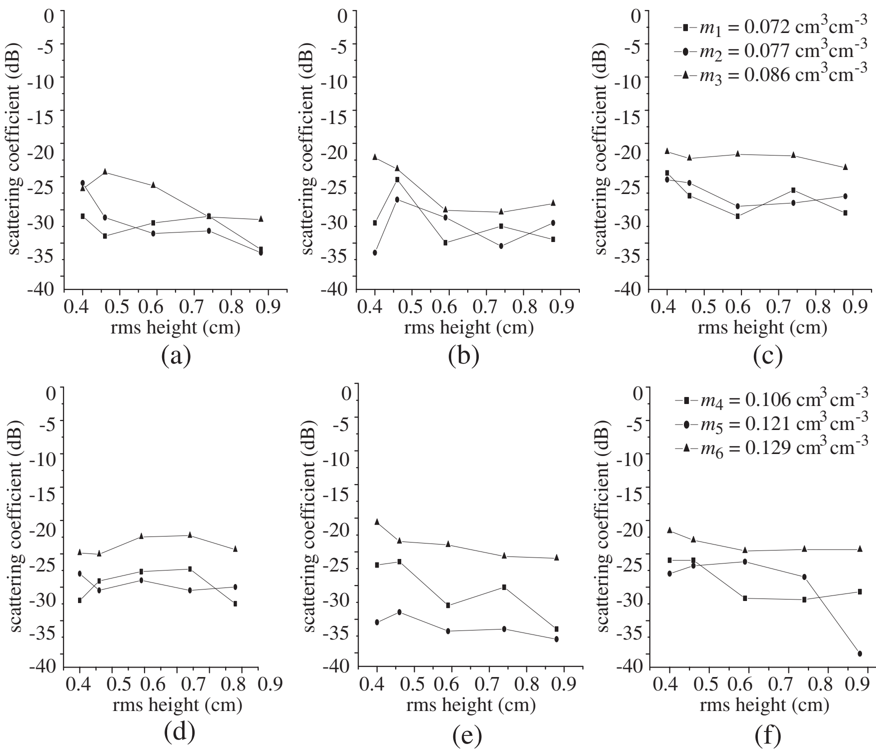

(a) (b) (c)
(d) (e) (f)

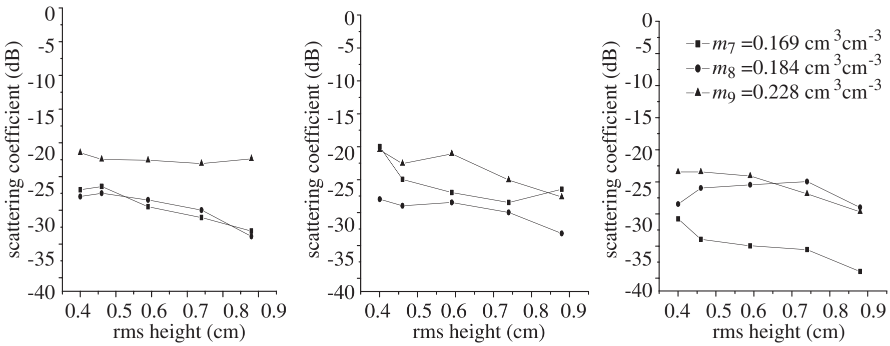

Figure 4. (a)–(c) Response of scattering coefficient with rms height at correlation length 2.97 cm, 2.64 cm and 2.29 cm respectively at volumetric moisture content $m_1 = 0.072\,\mathrm{cm}^3\,\mathrm{cm}^{-3}$, $m_2 = 0.077\,\mathrm{cm}^3\,\mathrm{cm}^{-3}$, $m_3 = 0.086\,\mathrm{cm}^3\,\mathrm{cm}^{-3}$. (d)–(f) Response of scattering coefficient with rms height at correlation length 2.15 cm, 2.02 cm and 1.86 cm respectively at volumetric moisture content $m_4 = 0.106\,\mathrm{cm}^3\,\mathrm{cm}^{-3}$, $m_5 = 0.121\,\mathrm{cm}^3\,\mathrm{cm}^{-3}$, $m_6 = 0.129\,\mathrm{cm}^3\,\mathrm{cm}^{-3}$. (g)–(i) Response of scattering coefficient with rms height at correlation length 1.72 cm, 1.60 cm and 1.51 cm respectively at volumetric moisture content $m_7 = 0.169\,\mathrm{cm}^3\,\mathrm{cm}^{-3}$, $m_8 = 0.184\,\mathrm{cm}^3\,\mathrm{cm}^{-3}$, $m_9 = 0.228\,\mathrm{cm}^3\,\mathrm{cm}^{-3}$.

Similar observations can be made from Figures 4(g)–(i), where σ° response at three different moisture levels (i.e., $m_7 = 0.169\,\mathrm{cm}^3\,\mathrm{cm}^{-3}$, $m_8 = 0.184\,\mathrm{cm}^3\,\mathrm{cm}^{-3}$ and $m_9 = 0.228\,\mathrm{cm}^3\ \mathrm{cm}^{-3}$) at three different correlation lengths (i.e., 1.72 cm, 1.60 cm and 1.51 cm) has been studied. At higher correlation length of 1.72 cm,response of σ° is irregular for lower moisture levels (i.e., m_7 and m_8) and approaches nearly same values, alternatively σ° response at $m_9 = 0.228\,\mathrm{cm}^3\,\mathrm{cm}^{-3}$ is regular and varies slightly with increase in s from 0.4 cm to 0.88 cm (Figure 4(g)). As correlation length lowers from 1.72 cm to 1.51 cm, an irregularity in σ° response is observed.

From above analysis it can thus be concluded that combination of higher moisture level with higher correlation length may be suitable for studying the effect of increasing rms height on scattering coefficient. As on one hand, the higher moisture levels with lower values of correlation length, i.e., l_8 and l_9 are undistinguishable for studying the effect of increasing s on σ°, so on the other hand, higher values of correlation length, i.e., l_1 and l_2 with moisture levels lower than $0.106\,\mathrm{cm}^3\,\mathrm{cm}^{-3}$ are also not suitable for the purpose.

As correlation length is decreased (i.e., roughness in horizontal direction increases) keeping rms height same (i.e., roughness in vertical direction remains unchanged), it is observed that dynamic range of VV decreases with increasing moisture content. This effect is more obvious at moderate correlation lengths. As roughness increases in horizontal direction, i.e., l becomes small, VV interacts more with the vertical component of the surface and results in fall of the dynamic range. A smooth soil surface corresponds generally to a small value of s and a large value of l [19]. Since, we have considered rms height from 0.4–0.88 cm. The smallest s values with larger correlation lengths represent a smooth surface which may be the cause of discrepancy in dynamic ranges at l_1 and l_2.

4.2. Retrieval of Roughness Parameter s, l and Moisture Content m_v

Higher incidence angles (i.e., greater than 40°) are found to be more sensitive for studying the effect of roughness and moisture content at X band for a bistatic case [5]. From Section 4.1, 60° is chosen as the best incidence angle for the analysis. Genetic algorithm has been used as an optimization technique for retrieving s and m_v from the cost function created using experimental and modeled scattering coefficient in VV polarization (Section 3.3). A good estimation of parameters has been obtained with error ranging from 0.1571–0.2201 for s, 0.0097–0.3536 for l and 0.0001–1.0830 for m_v.

Figure 5(a) shows the plot of observed moisture content vs. retrieved moisture content for different fields. Moisture content for fields with lower and moderate moisture content are more precisely predicted as compared to fields with higher moisture content. Figures 5(b) and 5(c) display the plot of observed rms height vs. retrieved rms height and observed correlation length vs. retrieved correlation length respectively. Deviation in retrieved s values from the observed ones is higher for fields F_1–F_5, i.e., the fields with lower moisture content and higher correlation lengths. Fields with moderate moisture content and moderate correlation length are found to be best for retrieving s. On the other hand, correlation length is retrieved with higher accuracy for all the fields.

Error in estimating m_v w.r.t. rms slope is given in Table 4. Rms slope varies as correlation length decreases from $l_1 = 2.97\,\text{cm}$ to $l_9 = 1.51\,\text{cm}$ with s remaining same for each set (i.e., $s_1 = 0.40\,\text{cm}$, $s_2 = 0.46\,\text{cm}$, $s_3 = 0.59\,\text{cm}$, $s_4 = 0.74\,\text{cm}$ and $s_5 = 0.88\,\text{cm}$).It is obvious from table that rms error tends to increase for higher slopes as we move from l_1 to l_9. Thus, we can conclude that for surfaces with higher rms slopes (for $s_i/l_7, s_i/l_8$ and s_i/l_9) moisture content is

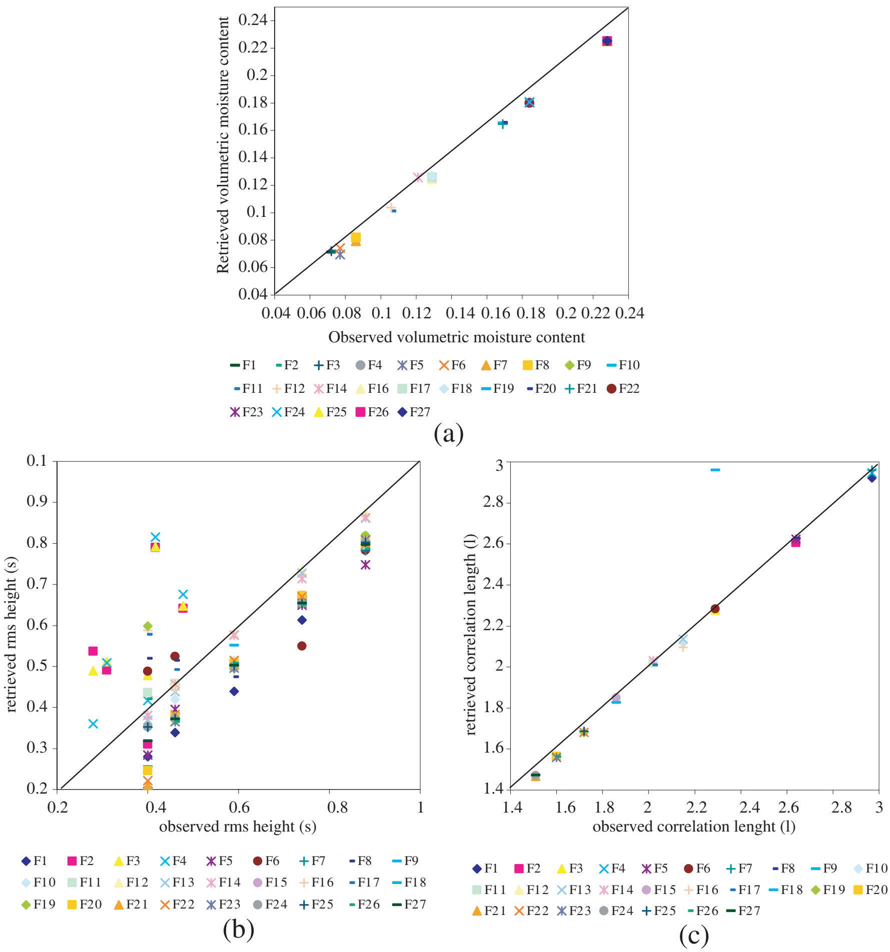

Figure 5. (a) Observed volumetric moisture content vs. retrieved volumetric content at different fields. (b) Observed rms height (in cm) vs. retrieved rms height at different fields. (c) Observed correlation length (in cm) vs. retrieved correlation length at different fields.

retrieved with less precision as compared to surfaces with lower rms slopes. Furthermore we can say that correlation lengths ($l_1 = 2.97$ cm–$l_6 = 1.86$ cm) are more effective for retrieving moisture content m_v from $0.072\,\mathrm{cm}^3\,\mathrm{cm}^{-3}$ upto $0.129\,\mathrm{cm}^3\,\mathrm{cm}^{-3}$.

Table 4. Rms error in estimating volumetric moisture content at different rms slopes. Where $s_{i \to 1 \text{ to } 5}$ for each correlation length.

Rms error	s_i/l_1	Rms error	s_i/l_2	Rms error	s_i/l_3
0.0059	0.135	0.0090	0.152	0.0087	0.175
0.2453	0.155	0.0074	0.174	0.0084	0.201
0.0065	0.199	0.0061	0.223	0.3505	0.258
0.2407	0.249	0.0061	0.280	0.0078	0.323
0.0063	0.296	0.0063	0.333	0.0061	0.384
	s_i/l_4		s_i/l_5		s_i/l_6
0.0144	0.186	0.0298	0.195	0.0126	0.215
0.0239	0.214	0.1570	0.224	0.0134	0.247
0.0253	0.274	0.0362	0.288	0.0163	0.317
0.0307	0.344	0.0383	0.361	0.0248	0.398
0.3593	0.409	0.0408	0.429	0.0336	0.473
	s_i/l_7		s_i/l_8		s_i/l_9
0.8546	0.233	0.8553	0.250	0.8562	0.265
0.8522	0.267	0.8601	0.288	0.8547	0.305
0.8540	0.343	0.8556	0.369	0.8547	0.391
0.8574	0.430	0.8551	0.463	0.8551	0.490
0.8582	0.512	0.8570	0.550	0.8576	0.583

5. CONCLUSION

An extensive data set on the various combinations of moisture levels and roughness parameters (s and l) in specular direction at X band (10 GHz) has been thoroughly investigated. Soil parameters (s, l and m_v) were retrieved using stationary phase approximation. Role of correlation length is well examined for specular scattering and it is observed that while considering the correlation length, moisture content from $0.072\,\text{cm}^3\,\text{cm}^{-3}$–$0.129\,\text{cm}^3\,\text{cm}^{-3}$ is retrieved with a good agreement whereas for higher moisture content ($0.169\,\text{cm}^3\,\text{cm}^{-3}$–$0.228\,\text{cm}^3\,\text{cm}^{-3}$) roughness effect is prominent. Throughout the study, correlation length and moisture content has been varied keeping constant range for rms height (i.e., 0.40 cm–0.88 cm). On varying correlation length, rms slope changes. From results it can be concluded that for moderately rougher surfaces an increase in correlation length decreases the accuracy in estimation of moisture contents. This study signifies the importance of correlation length as a roughness parameter alongwith rms height for soil moisture retrieval modeling with specular scattering.

APPENDIX A.

Fields	Different combinations of (m_v, l and s)				
$F_1(m_1,l_1,s_k)$	(0.072,2.97,0.40)	(0.072,2.97,0.46)	(0.072,2.97,0.59)	(0.072,2.97,0.74)	(0.072,2.97,0.88)
$F_2(m_1,l_2,s_k)$	(0.072,2.64,0.40)	(0.072,2.64,0.46)	(0.072,2.64,0.59)	(0.072,2.64,0.74)	(0.072,2.64,0.88)
$F_3(m_1,l_3,s_k)$	(0.072,2.29,0.40)	(0.072,2.29,0.46)	(0.072,2.29,0.59)	(0.072,2.29,0.74)	(0.072,2.29,0.88)
$F_4(m_2,l_1,s_k)$	(0.077,2.97,0.40)	(0.077,2.97,0.46)	(0.077,2.97,0.59)	(0.077,2.97,0.74)	(0.077,2.97,0.88)
$F_5(m_2,l_2,s_k)$	(0.077,2.64,0.40)	(0.077,2.64,0.46)	(0.077,2.64,0.59)	(0.077,2.64,0.74)	(0.077,2.64,0.88)
$F_6(m_2,l_3,s_k)$	(0.077,2.29,0.40)	(0.077,2.29,0.46)	(0.077,2.29,0.59)	(0.077,2.29,0.74)	(0.077,2.29,0.88)
$F_7(m_3,l_1,s_k)$	(0.086,2.97,0.40)	(0.086,2.97,0.46)	(0.086,2.97,0.59)	(0.086,2.97,0.74)	(0.086,2.97,0.88)
$F_8(m_3,l_2,s_k)$	(0.086,2.64,0.40)	(0.086,2.64,0.46)	(0.086,2.64,0.59)	(0.086,2.64,0.74)	(0.086,2.64,0.88)
$F_9(m_3,l_3,s_k)$	(0.086,2.29,0.40)	(0.086,2.29,0.46)	(0.086,2.29,0.59)	(0.086,2.29,0.74)	(0.086,2.29,0.88)
$F_{10}(m_4,l_4,s_k)$	(0.106,2.15,0.40)	(0.106,2.15,0.46)	(0.106,2.15,0.59)	(0.106,2.15,0.74)	(0.106,2.15,0.88)
$F_{11}(m_4,l_5,s_k)$	(0.106,2.02,0.40)	(0.106,2.02,0.46)	(0.106,2.02,0.59)	(0.106,2.02,0.74)	(0.106,2.02,0.88)
$F_{12}(m_4,l_6,s_k)$	(0.106,1.86,0.40)	(0.106,1.86,0.46)	(0.106,1.86,0.59)	(0.106,1.86,0.74)	(0.106,1.86,0.88)
$F_{13}(m_5,l_4,s_k)$	(0.121,2.15,0.40)	(0.121,2.15,0.46)	(0.121,2.15,0.59)	(0.121,2.15,0.74)	(0.121,2.15,0.88)
$F_{14}(m_5,l_5,s_k)$	(0.121,2.02,0.40)	(0.121,2.02,0.46)	(0.121,2.02,0.59)	(0.121,2.02,0.74)	(0.121,2.02,0.88)
$F_{15}(m_5,l_6,s_k)$	(0.121,1.86,0.40)	(0.121,1.86,0.46)	(0.121,1.86,0.59)	(0.121,1.86,0.74)	(0.121,1.86,0.88)
$F_{16}(m_6,l_4,s_k)$	(0.129,2.15,0.40)	(0.129,2.15,0.46)	(0.129,2.15,0.59)	(0.129,2.15,0.74)	(0.129.,2.15,0.88)
$F_{17}(m_6,l_5,s_k)$	(0.129,2.02,0.40)	(0.129,2.02,0.46)	(0.129,2.02,0.59)	(0.129,2.02,0.74)	(0.129,2.02,0.88)
$F_{18}(m_6,l_6,s_k)$	(0.129,1.86,0.40)	(0.129,1.86,0.46)	(0.129,1.86,0.59)	(0.129,1.86,0.74)	(0.129.,1.86,0.88)
$F_{19}(m_7,l_7,s_k)$	(0.169,1.72,0.40)	(0.169,1.72,0.46)	(0.169,1.72,0.59)	(0.169,1.72,0.74)	(0.169,1.72,0.88)
$F_{20}(m_7,l_8,s_k)$	(0.169,1.60,0.40)	(0.169,1.60,0.46)	(0.169,1.60,0.59)	(0.169,1.60,0.74)	(0.169,1.60,0.88)
$F_{21}(m_7,l_9,s_k)$	(0.169,1.51,0.40)	(0.169,1.51,0.46)	(0.169,1.51,0.59)	(0.169,1.51,0.74)	(0.169,1.51,0.88)
$F_{22}(m_8,l_7,s_k)$	(0.184,1.72,0.40)	(0.184,1.72,0.46)	(0.184,1.72,0.59)	(0.184,1.72,0.74)	(0.184,1.72,0.88)
$F_{23}(m_8,l_8,s_k)$	(0.184,1.60,0.40)	(0.184,1.60,0.46)	(0.184,1.60,0.59)	(0.184,1.60,0.74)	(0.184,1.60,0.88)
$F_{24}(m_8,l_9,s_k)$	(0.184,1.51,0.40)	(0.184,1.51,0.46)	(0.184,1.51,0.59)	(0.184,1.51,0.74)	(0.184,1.51,0.88)
$F_{25}(m_9,l_7,s_k)$	(0.228,1.72,0.40)	(0.228,1.72,0.46)	(0.228,1.72,0.59)	(0.228,1.72,0.74)	(0.228,1.72,0.88)
$F_{26}(m_9,l_8,s_k)$	(0.228,1.60,0.40)	(0.228,1.60,0.46)	(0.228,1.60,0.59)	(0.228,1.60,0.74)	(0.228,1.60,0.88)
$F_{27}(m_9,l_9,s_k)$	(0.228,1.51,0.40)	(0.228,1.51,0.46)	(0.228,1.51,0.59)	(0.228,1.51,0.74)	(0.228,1.51,0.88)

†where for field $F_n(m_i, l_j, s_k)$ n corresponds to the no. of field, $n \to 1$ to 27 and $k \to 1$ to 5 for each field.

‡$F_{n\to 1 \text{ to } 3}$ $(m_{i=1},\ l_{j\to 1 \text{ to } 3},\ s_{k\to 1 \text{ to } 5})$; $F_{n\to 4 \text{ to } 6}$ $(m_{i=2},\ l_{j\to 1 \text{ to } 3},\ s_{k\to 1 \text{ to } 5})$; $F_{n\to 7 \text{ to } 9}$ $(m_{i=3},\ l_{j\to 1 \text{ to } 3},\ s_{k\to 1 \text{ to } 5})$; $F_{n\to 10 \text{ to } 12}$ $(m_{i=4},\ l_{j\to 4 \text{ to } 6},\ s_{k\to 1 \text{ to } 5})$; $F_{n\to 13 \text{ to } 15}$ $(m_{i=5},\ l_{j\to 4 \text{ to } 6},\ s_{k\to 1 \text{ to } 5})$; $F_{n\to 16 \text{ to } 18}$ $(m_{i=6},\ l_{j\to 4 \text{ to } 6},\ s_{k\to 1 \text{ to } 5})$; $F_{n\to 19 \text{ to } 21}$ $(m_{i=7},\ l_{j\to 7 \text{ to } 9},\ s_{k\to 1 \text{ to } 5})$; $F_{n\to 22 \text{ to } 24}$ $(m_{i=8},\ l_{j\to 7 \text{ to } 9},\ s_{k\to 1 \text{ to } 5})$ and $F_{n\to 25 \text{ to } 27}$ $(m_{i=9},\ l_{j\to 7 \text{ to } 9},\ s_{k\to 1 \text{ to } 5})$.

APPENDIX B.

Stationary phase approximation in specular direction:

The vector formulation of the Kirchoff method is based upon the vector second Green's theorem, which states that the scattered field at any point within a source free region bounded by a closed surface can be expressed in terms of the tangential fields on the surface. A mathematical statement of this fact is as follows (refer for the derivation, appendix 12J of [1]):

$$\vec{E}^s = K\hat{n}_s \times \int \left[\hat{n} \times \vec{E} - \eta_s \hat{n}_s \times \left(\hat{n} \times \vec{H}\right)\right] e^{jk_s \vec{r}\cdot\hat{n}_s} ds \tag{B1}$$

where

$K = -jk_s e^{-jk_s R_0}/4\pi R_0$,

$\hat{n}_s$ = unit vector in the scattered direction,

$\hat{n}$ = unit vector normal to interface inside the medium in which scattering is considered,

η_s = intrinsic impedance of the medium in which $\vec{E}^s$ is evaluated,

k_s = wave number of the medium in which $\vec{E}^s$ is evaluated,

R_0 = range from the center of the illuminated area to the point of observation,

$\vec{E}, \vec{H}$ = total electric and magnetic fields on the interface.

To determine tangential fields $\hat{n} \times \vec{E}$ and $\hat{n} \times \vec{H}$ on the interface, incident wave is assumed to be:

$$\vec{E}^i = \hat{a}E_0 \exp\left(-jk\hat{n}_i \cdot \vec{r}\right) \tag{B2}$$

Figure B1 shows the geometry of the surface-scattering problem. Details of the figure can be obtained from [1].

Tangential fields $\hat{n} \times \vec{E}$ and $\hat{n} \times \vec{H}$ on the interface are determined as given by Eqs. (12.15) and (12.16) in Ulaby, 1982 [1]. Using both fields in Eq. (B1), the scattered field in medium 1 is given as:

$$E^s = K\hat{n}_1 \times \int \left[\hat{n}_1 \times E - \eta_1 \hat{n}_s \times (\hat{n}_1 \times H)\right] \exp\left[jk_1\left(\hat{n}_s - \hat{n}_i\right)\cdot r'\right] ds' \tag{B3}$$

where,

$\hat{n}_i$ =the unit vector in the incident direction,

$\hat{n}_s$ =the unit vector in scattered direction,

k_1 =the wave number in medium one,

η_1 =the intrinsic impedance of medium 1.

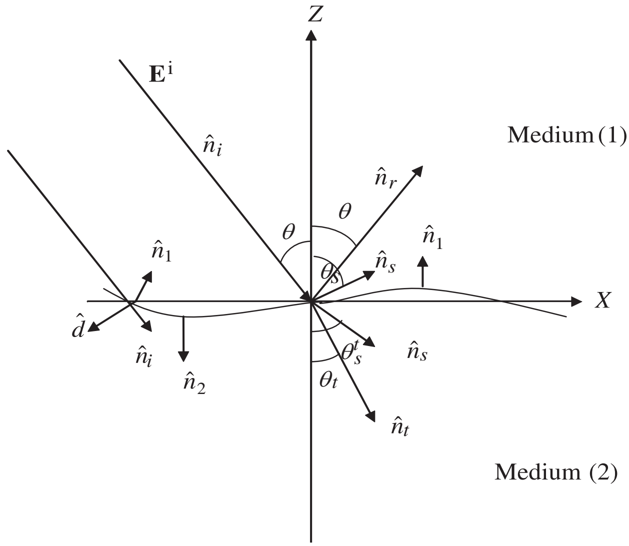

Figure B1. Geometry of the scattering problem.

Reflected Bistatic scattering coefficient in medium 1 is given as:

$$\sigma_{pq}^{0} = \frac{\left(kq\left|U_{pq}\right|\right)^2}{2q_z^4\sigma^2\left|\rho''(0)\right|}\exp\left[-\frac{q_x^2+q_y^2}{2q_z^4\sigma^2\left|\rho''(0)\right|}\right] \tag{B4}$$

where $p \rightarrow$ polarization of transmitted wave, $q \rightarrow$ polarization of received wave, $\sigma^2\left|\rho''(0)\right|$ is mean square slope of the surface, U_{pq} is complex coefficient that depends on polarization, dielectric constant and local incidence angle.

Angular set for bistatic geometry is θ_i, θ_s and φ_Δ, where $\varphi_\Delta = \varphi_s - \varphi_i$, θ_i is the local incidence angle, θ_s being scattered angle, φ_i is the azimuthal angle of incidence wave and φ_s being of scattered wave.

The approximation relations from the phase term, Q of Eq. (B3) are obtained. Q is defined as:

$$Q = k_1\left(\hat{n}_s - \hat{n}_i\right)\cdot r' \equiv q_x x' + q_y y' + q_z z' \tag{B5}$$

where:

$$\hat{n}_s = \hat{x}\sin\theta_s\cos\phi_s + \hat{y}\sin\theta_s\sin\phi_s + \hat{z}\cos\theta_s \tag{B5a}$$
$$\hat{n}_i = \hat{x}\sin\theta_i\cos\phi_i + \hat{y}\sin\theta_i\sin\phi_i + \hat{z}\cos\theta_i \tag{B5b}$$
$$q_x = k_1\left(\sin\theta_s\cos\phi_s - \sin\theta_i\cos\phi_i\right) \tag{B5c}$$
$$q_y = k_1\left(\sin\theta_s\sin\phi_s - \sin\theta_i\sin\phi_i\right) \tag{B5d}$$
$$q_z = k_1\left(\cos\theta_s + \cos\theta_i\right) \tag{B5e}$$

$$q^2 = \sqrt{q_x^2 + q_y^2 + q_z^2} \tag{B5f}$$

For Bistatic specular case: $\theta_s = \theta_i = \theta$, φ_Δ =0° which implies:

$$q_x^2 + q_y^2 = 0 \tag{B6}$$

As mentioned in [4, 6] for specular direction U_{pq} takes the form

$$\begin{aligned} U_{hh}(\theta) &= 2R_h(\theta)\cos\theta \\ U_{hv}(\theta) &= 0 \\ U_{vv}(\theta) &= -2R_v\cos\theta \end{aligned} \tag{B7}$$

where,

$$R_h = \frac{\cos\theta - \sqrt{\varepsilon - \sin^2\theta}}{\cos\theta + \sqrt{\varepsilon + \sin^2\theta}} \ \& \ R_v = \frac{\varepsilon\cos\theta - \sqrt{\varepsilon - \sin^2\theta}}{\varepsilon\cos\theta + \sqrt{\varepsilon + \sin^2\theta}} \tag{B8}$$

using above conditions Eq. (B4) reduces to:

$$\sigma_{pq}^0 = \frac{|U_{pq}|^2}{2\sigma^2\,|\rho''(0)|} \tag{B9}$$

ACKNOWLEDGMENT

Authors are thankful to Physical Research Lab, Ahmedabad, India and Department of Science and Technology, India for providing funds for this work.

REFERENCES

1. Ulaby, F. T., R. K. Moore, and A. K. Fung, *Microwave Remote Sensing: Active and Passive*, Vol. 2–3, Addison-Wesley Publishing company, Reading, MA, USA, 1982.
2. Oh, Y., K. Sarabandi, and F. T. Ulaby, "An empirical model and an inversion technique for radar scattering from bare soil surfaces," *IEEE Transactions on Geoscience and Remote Sensing*, Vol. 30, 370–381, 1992.
3. Dubois, P., J. Van Zyl, and T. Engman, "Measuring soil moisture with imaging radars," *IEEE Transations on Geoscience and Remote Sensing*, Vol. 33, 915–926, 1995.
4. Ceraldi, E., G. Franceschetti, A. Iodice, and D. Riccio, "Estimating the soil dielectric constant via scattering measurements along the specular direction," *IEEE Transactions on Geoscience and Remote Sensing*, Vol. 43, No. 2, 295–205, 2005.

5. Singh, D. and V. Dubey, "Microwave bistatic polarization measurements for retrieval of soil moisture using an incidence angle approach," *Journal of Geophysics and Engineering*, Vol. 4, 75–82, 2007.
6. Khadra, K. B., "Surface parameter estimation using bistatic polarimetric X-band measurements," Ph.D. thesis, German Aerospace Centre (DLR), Institute of Radio Frequency Technology, Oberpfaffenhofen, Germany, 2008.
7. Roo, R. D., "Theory and measuerement of bistatic scattering of X band microwaves from rough dielectric surfaces," Ph.D. thesis, Michigan University, USA, 1996.
8. Macelloni, G., G. Nesti, P. Pampaloni, S. Sigismmondi, D. Tarchi, and S. Lolli, "Experimental validation of surface scattering and emission models", *IEEE Transations on Geoscience and Remote Sensing*, Vol. 38, No. 1, 203–244, 2000.
9. Singh, D., "Polarization discrimination ratio approach to retrieve bare soil moisture at X-band," *IEEE International Geoscience and Remote Sensing Symposium Proceedings*, 408–411, Seoul, Korea, Jul. 25–29, 2005.
10. Zhixiong, L., C. Nan, U. D. Perdok, and W. B. Hoogmoed, "Characterization of soil profile roughness," *Boisystems Engineering*, Vol. 91, 369–377, 2005.
11. Yisok, O. H. and J. Y. Hong, "Effect of surface profile length on the backscattering coefficients of bare surfaces," *IEEE Transactions on Geoscience and Remote Sensing*, Vol. 45, 632–638, 2002.
12. Jun, Z. and S. Donglin, "Scattering signatures analysis using genetic algorithm," *Asia-Pacific Conference on Environmental Electromagnetics, CEEM'2003*, 514–517, Nov. 4–7, 2003.
13. Curie, N. C., *Radar Reflectivity Measurement: Techniques and Applications*, Artech House, Norwood, MA, 1989.
14. Kuria, D., L. Hui, T. Koike, H. Tsutsui, and T. Graf, "Multifrequency response to periodic roughness," *IEEE International Geoscience and Remote Sensing Symposium Proceedings*, 1744–1747, Denver, Colorado, Jul. 31–Aug. 4, 2006.
15. Rahman, M. M., M. S. Moran, D. P. Thoma, R. Bryant, E. E. Sano, C. D. Holifield Collins, S. Skirvin, C. Kreshner, and B. J. Orr, "A description of roughness correlation length for parameterizing backscatter models," *IJRS*, Vol. 28, 3995–4012, 2007.
16. Zribi, M., N. Baghdadi, N. Holah, and O. Fafin, "New

methodology for soil surface moisture estimation and its application to ENVISAT-ASAR multi-incidence data inversion," *Remote Sensing of Environment*, Vol. 96, 485–496, 2005.

17. Hajnsek, I., "Inversion of surface parameters using polarimetric SAR," Ph.D. thesis, Friedrich-Schilller university Jena, Institute of geography, Oberpfaffenhofen, Germany, 2001.
18. Mardle, S. and S. Pascoe, "An overview of genetic algorithms for the solution of optimization problems," *CHEER*, Vol. 13, 1999.
19. Zribi, M. and M. Dechambre, "A new empirical model to retrieve soil moisture and roughness from C-band radar data," *Remote Sensing of Environment*, Vol. 84, 42–52, 2002.
20. Mittal, G. and D. Singh, "Microwave response on surface roughness at X-band for remote sensing," *ICRS* (*International Centre of Remote Sensing*) *Conference*, Jodhpur (Rajasthan), India, Feb. 27–29, 2008.